ACCOUNTS
of chemical research

Photonic Nanowires: From Subwavelength Waveguides to Optical Sensors

XIN GUO,[†] YIBIN YING,[‡] AND LIMIN TONG*,[†]

[†]*State Key Laboratory of Modern Optical Instrumentation, Department of Optical Engineering and* [‡]*College of Biosystems Engineering and Food Science, Zhejiang University, Hangzhou, Zhejiang 310027, China*

RECEIVED ON SEPTEMBER 29, 2013

CONSPECTUS

Nanowires are one-dimensional (1D) nanostructures with comparatively large aspect ratios, which can be useful in manipulating electrons, photons, plasmons, phonons, and atoms for numerous technologies. Among various nanostructures for low-dimensional photonics, the 1D nanowire is of great importance owing to its ability to route tightly confined light fields in single-mode with lowest space and material requirements, minimized optical path, and high mechanical flexibilities. In recent years, nanowire photonics have increasingly been attracting scientists' interests for both fundamental studies and technological applications because 1D nanowires have more favorable properties than many other structures, such as 0D quantum dots (QDs) and 2D films.

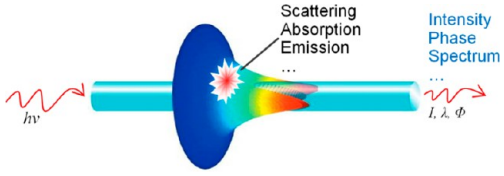

As subwavelength waveguides, free-standing nanowires fabricated by either chemical growth or physical drawing techniques surpass nanowaveguides fabricated by almost all other means in terms of sidewall smoothness and diameter uniformity. This conveys their low waveguiding losses. With high index contrast (typically higher than 0.5) between the core and the surrounding or with surface plasmon resonance, a nanowire can guide light with tight optical confinement. For example, the effective mode area is less than $\lambda^2/10$ for a dielectric nanowire or less than $\lambda^2/100$ for a metal nanowire, where λ is the vacuum wavelength of the light. As we increase the wavelength-to-diameter ratio (WDR) of a nanowire, we can enlarge the fractional power of the evanescent fields in the guiding modes to over 80% while maintaining a small effective mode area, which may enable highly localized near-field interaction between the guided fields and the surrounding media. These favorable properties have opened great opportunities for optical sensing on the single-nanowire scale. However, several questions arise with ongoing research. With a deep-subwavelength cross-section, how can we efficiently couple light into a single nanowire? How can we fabricate a nanowire with low optical loss? How can we activate a passive nanowire for optical sensing? And lastly, how can we adapt mature optical measurement technology onto a nanowire?

In this Account, we highlight our initial attempts to address the above-mentioned challenges. First, we introduce the fabrication and functionalization of low-loss photonic nanowires. We show that nanowires fabricated by either top-down physical drawing (e.g., for amorphous nanowires) or bottom-up chemical growth (e.g., for crystalline nanowires) can yield excellent geometric and structural uniformities with surface roughness down to atomic level and minimize the scattering loss for subwavelength optical or plasmonic waveguiding. Then, relying on a near-field fiber-probe micromanipulation, we demonstrate optical launching of single nanowires by evanescent coupling, with coupling efficiency up to 90% for dielectric nanowires and 80% for plasmonic nanowires. Third, we discuss the waveguiding properties of nanowires and emphasize their outstanding capability of waveguiding tightly confined optical fields with high fractional evanescent fields. In addition, we briefly show a balance between the loss, confinement, and bandwidth in a waveguiding nanowire. Fourthly, we present promising approaches to single-nanowire optical sensors. By measuring optical absorption or spectral transmission of a nanowire and activating nanowires with sensitive dopants, we demonstrate a single-nanowire optical sensor with high sensitivity, fast response, and low optical power. This may lead to a novel platform for optical sensing at nanoscale. Finally, we conclude with an outlook for future challenges in the light manipulation and sensing applications of photonic nanowires.

1. Introduction

As one-dimensional (1D) nanostructures with relatively large aspect ratios, nanowires are capable of manipulating electrons, photons, plasmons, phonons, and atoms on the nanoscale for various possibilities.[1−4] Among the broad coverage of nanowire research, nanowire photonics has

Published on the Web 12/31/2013 www.pubs.acs.org/accounts
10.1021/ar400232h

been attracting increasing interest for both fundamental studies and technological applications in recent years. For photonics, the 1D nanowire provides favorable properties over many other structures [e.g., 0D quantum dots (QDs) and 2D films]. First of all, a nanowire can handle light as a subwavelength waveguide within the visible to infrared spectral range, with tight optical confinement,[5] small footprint, and low optical power. Second, with a subwavelength transverse dimension, a nanowire can guide light with a large fractional power outside as evanescent waves,[5] which greatly facilitate the near-field interaction of the guided light and the surrounding materials. Third, since the mass of a free-standing nanowire is very low, the momentum change of the guided light (e.g., redirection, absorption, or radiation of light) is strong enough to induce mechanical movement of the nanowire,[6] suggesting an alternative approach to optical sensing via mechanical displacement, as well as nanoscale optomechanical components and devices.[7] Finally, a nanowire usually exhibits much higher mechanical strength and pliability than its bulk counterpart[8,9] and is visible under an optical microscope, which greatly facilitates the micromanipulation of nanowires into desired geometries and positions.

A nanoscale sensor is one of the most promising applications of nanowires. So far, a variety of miniaturized sensing platforms based on electrical conductivity of single nanowires have been successfully demonstrated.[10,11] Compared with the electrical approach, optical sensing may offer higher sensitivity, faster response, better immunity to electromagnetic interference, and safer operation in an explosive or combustive atmosphere, as well as more options for signal retrieval from optical intensity, spectrum, phase, polarization, and fluorescence lifetime.[12] However, replacing electrical current with a light beam in a nanowire for optical sensing confronts some major challenges: First, how can we efficiently couple light into a single nanowire. Unlike the current in copper wires that can be put through by a simple touch, optical connection (e.g., between optical fibers) usually requires elaborated alignment. Second, how can we realize low waveguiding loss in a nanowire? Radiation loss (e.g., from defect-induced scattering) may cause evident background noise and deterioration in coherence and polarization that are critical for phase-sensitive optical detection. Moreover, high loss leads to weak transmission, which may in turn increase the photodetection time and slow the response of the sensor. Third, how can we activate a nanowire for optical sensing while maintaining its simple 1D structure? Usually, a nanowire acts as a passive waveguide. Additional functionalization is highly desired to make it sensitive to particular samples. Finally, how can we adapt the mature optical metrology for a nanowire to make the nanowire sensor more powerful and versatile?

This Account focuses on our recent research on photonic nanowires from subwavelength waveguiding to optical sensing, with emphases on possible solutions to the above-mentioned challenges. First, we introduce fabrication and functionalization of low-loss photonic nanowires. Then, recent progress on efficient launching and subwavelength waveguiding of single nanowires is summarized and discussed. In section5, after a brief discussion on the principles of nanowire optical sensing, we present promising approaches to single-nanowire optical sensors to details. Finally, we conclude with an outlook on the future opportunities and challenges in light manipulation and sensing applications of photonic nanowires.

2. Fabrication of Photonic Nanowires

Typical materials for 1D photonic nanowires can be categorized into three general classes: dielectric that is usually amorphous (e.g., silica glass, polystyrene), semiconductor with crystalline structure (e.g., ZnO, CdS), and metal (e.g., Ag, Au).

For amorphous dielectric materials, a top-down physical drawing process is usually preferred. Taper drawing a molten glass fiber at a speed around 1 mm/s can yield a glass nanowire (also called a nanofiber) with diameter down to 50 nm and large length (Figure 1a,b).[13] Because of the surface tension, the as-drawn nanowire shows a circular cross-section (Figure 1c), an extremely smooth surface (surface roughness down to 0.2 nm) (Figure 1d), and excellent diameter uniformity.[13−15] Similarly, optical-quality polymer nanowires can be obtained by drawing solvent polymer solutions at room temperature (Figure 1e)[16−18] or molten polymers.[19] Compared with other fabrication techniques such as electron beam lithography or chemical growth for glass nanowires[20,21] and electrospinning for polymer nanowires,[22,23] physical drawing methods yield nanowires with much better qualities in terms of surface smoothness and diameter uniformity, which enables low-loss optical waveguiding in these 1D nanostructures.

For crystalline semiconductors, bottom-up syntheses such as chemical growth[24] have proven very successful for fabricating nanowires with crystalline structures, excellent surface quality, and high diameter uniformity (Figure 1f).[8,25] As a crystal growth process, the growth rate for single nanowires is much slower (e.g., 50 nm/s) than the top-down physical drawing (e.g., 1 mm/s). However, it grows hundreds

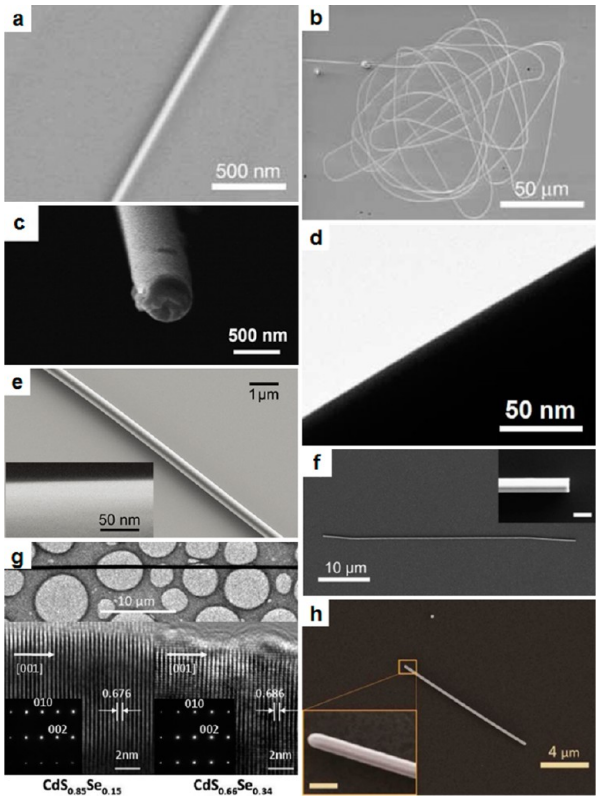

FIGURE 1. Electron microscope images of some typical 1D photonic nanowires. (a) A 50 nm diameter silica nanowire. Adapted from ref 13 with permission. Copyright 2003 Nature Publishing Group. (b) A 4 mm length 260 nm diameter coiled silica nanowire. Adapted from ref 13 with permission. Copyright 2003 Nature Publishing Group. (c) Cross-section of a 480 nm diameter silica nanowire. Adapted from ref 14 with permission. Copyright 2008 Elsevier. (d) Sidewall of a 210 nm diameter phosphate glass nanowire. Adapted from ref 15 with permission. Copyright 2006 Optical Society of America. (e) A 400 nm diameter polystyrene (PS) nanowire doped with rhodamine B (RhB). Adapted from ref 18 with permission. Copyright 2010 American Chemical Society. (f) A 200 nm diameter CdSe nanowire. Adapted from ref 25 with permission. Copyright 2011 American Chemical Society. (g) A CdSSe nanowire (above) and its corresponding high-resolution transmission electron microscopy (HRTEM) images and selected area electron diffraction (SAED) patterns taken from several representative regions along its length (below). Adapted from ref 27 with permission. Copyright 2011 American Chemical Society. (h) A 260 nm diameter Ag nanowire. Inset scale bar, 400 nm. Adapted from ref 33 with permission. Copyright 2010 Optical Society of America.

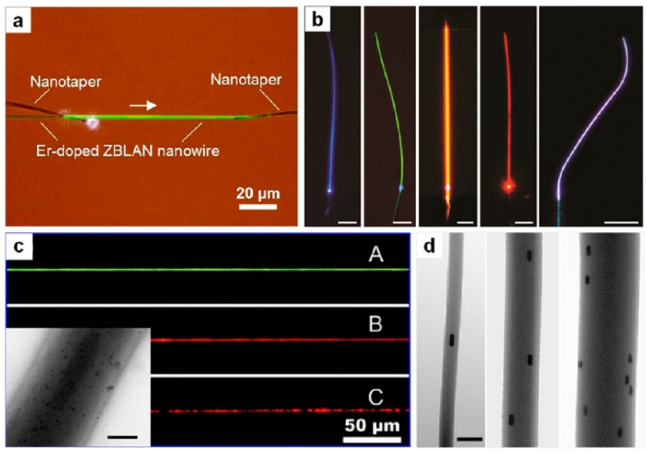

FIGURE 2. Functionally doped photonic nanowires. (a) Photoluminescence (PL) image of a 320 nm diameter Er-doped ZBLAN ($53ZrF_4-20BaF_2-3.9LaF_3-3AlF_3-20NaF-0.1ErF_3$) glass nanowire excited by a 975 nm wavelength light. Adapted from ref 15 with permission. Copyright 2006 Optical Society of America. (b) PL images of photoexcited dye-molecule-doped polymer nanowires. Scale bars, 50 μm. Adapted from ref 18 with permission. Copyright 2010 American Chemical Society. (c) PL images of PS nanowires doped with CdSe QDs with different sizes. Inset, TEM image of a 280 nm diameter QD-doped PS nanowire. Inset scale bar, 100 nm. Adapted from ref 34 with permission. Copyright 2011 Wiley. (d) TEM images of Au-nanorod-doped polyacrylamide (PAM) nanowires with diameters of 150, 360, and 600 nm, respectively. Scale bar, 250 nm. Adapted from ref 35 with permission. Copyright 2012 American Chemical Society.

of thousands of nanowires at the same time, making it an efficient and high-yield fabrication method. Also, the controllable parameters during the growth procedure make the bottom-up growth a highly flexible technique for tailoring the bandgap structure [e.g., superlattice[26] and graded bandgap[27] (Figure 1g)] and geometry (e.g., nanowire taper, branch,[28] and comb[29]) of the semiconductor nanowire for photonic applications. In addition, nanowires grown by the bottom-up approach can be as thin as several nanometers, providing an opportunity to manifest evident quantum confinement effects[30] and modify photonic properties of the nanowires for light absorption and emission.

Typical materials for optical-frequency plasmonic applications are noble metals such as Au and Ag. Despite the high absorption, radiation loss originating from crystalline boundary scattering cannot be neglected, and metal nanowires with good crystalline integrity is usually desired for both localized and propagation surface plasmons.[31] Among various fabrication methods, seed-growth method is deemed the most successful technique for growing metal nanowires with smooth sidewalls, large length, high yield, and crystalline structures (Figure 1h).[32,33]

Two or more materials can be combined into a complex mixture for fabricating functionally activated photonic nanowires. Several approaches, including doping, blending, coating, and near-field coupling, can be used to incorporate exotic functional materials into nanowires. For example, by doping the starting material before nanowire drawing, our group incorporated a variety of functional dopants, including rare-earth ions (Figure 2a),[15] dye molecules (Figure 2b),[18] QDs (Figure 2c),[34] and metal nanoparticles (Figure 2d),[35] into photonic nanowires. Also, to functionalize the nanowire

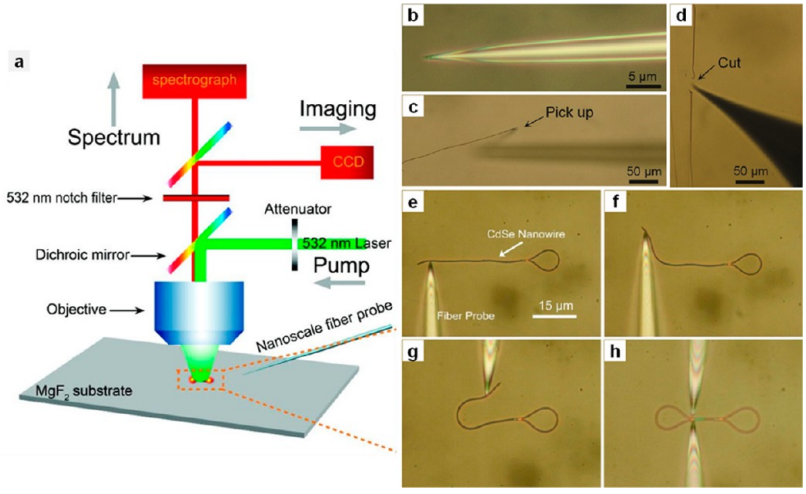

FIGURE 3. Micromanipulation of a single nanowire. (a) Schematic diagram of experimental setup. Adapted from ref 25 with permission. Copyright 2011 American Chemical Society. (b–h) Optical microscope images of (b) a fiber probe, (c) pick up, and (d) cut of a polymer nanowire (Panels b–d adapted from ref 18 with permission. Copyright 2010 American Chemical Society); and (e–h) fold one end of a CdSe nanowire into a loop (Panels e–h adapted from ref 25 with permission. Copyright 2011 American Chemical Society).

with subwavelength transverse dimension, active dopants do not always need to be physically doped inside or contacted with the nanowire but could be doped into the optical near field outside the nanowire (e.g., 100 nm away from the nanowire surface), as has been indicated in waveguiding nanofibers surrounded by QDs.[36] These complex-mixture nanowires not only expand the material diversity for 1D photonics, but also have opened new opportunities of waveguiding, localization, generation, and conversion of light for many applications including optical sensing, as discussed in sections 3 and 4.

3. Manipulation of Single Nanowires

3.1. Manipulation Systems. Micromanipulation is indispensable for shaping, positioning, and characterization of individual nanowires. Commercially available high-precision micromanipulators are usually designed for working in a SEM or a TEM, making it difficult to image the nanowire by optical means, which is highly desired for in situ optical characterization. A convenient approach is using tapered fiber probes for micromanipulation under an optical microscope in the open air (Figure 3a).[25] Typically, a nanowire longer than 2 μm can be clearly identified under an optical microscope. When equipped with a superlong-working-distance (SLWD) objective, the working distance of such a system (e.g., 6 mm for a 100× objective, 20 mm for a 20× objective) is large enough for single-nanowire micromanipulation. With fiber probes (tip size ~500 nm, Figures 3b,c) or tungsten STM probes (tip size <100 nm, Figure 3d) mounted on three-dimensional precision stages, nanowires can be individually picked up (Figure 3c), cut (Figure 3d), transferred, bent, and shaped (Figure 3e–h) with acceptable precision.[18,25]

3.2. Functional Assembly. Owing to their high strengths and pliabilities, as-fabricated nanowires can be manipulated into functional structures, for example, tying a nanowire into a microring for introducing optical resonance (Figure 4a),[13,14] assembling a nanowire into a Mach–Zehnder structure for introducing optical interference (Figure 4b),[37] folding one end of a nanowire into a Sagnac loop to obtain high reflectivity (Figure 4c),[25] and coupling dielectric and metal nanowires to realize a hybrid photon–plasmon nanowire structure (Figure 4d).[38] The structural assembly offers an opportunity to incorporate mature optical technology into nanowires while maintaining small footprints.

3.3. Optical Launching of Single Nanowires. Due to its deep-subwavelength cross-section, a nanowire is difficult to launch by conventional lens-focused coupling. The strong evanescent fields of a nanowire propose a possible approach to sending light into a single nanowire. As shown in Figure 5a, when a nanowire is brought into contact with a fiber probe via micromanipulation, light can be evanescently coupled from a fiber probe into a nanowire.[17] Despite the material index difference (e.g., 1.46 for silica vs 2.08 for telluride), high efficiency (e.g., 92% from a 450 nm diameter silica nanowire to a 200 nm diameter tellurite nanowire) can be obtained when the effective indices of both waveguides are matched.[39] Using end scattering for further compensation of the momentum mismatch, we have also used this technique to launch plasmonic nanowires with

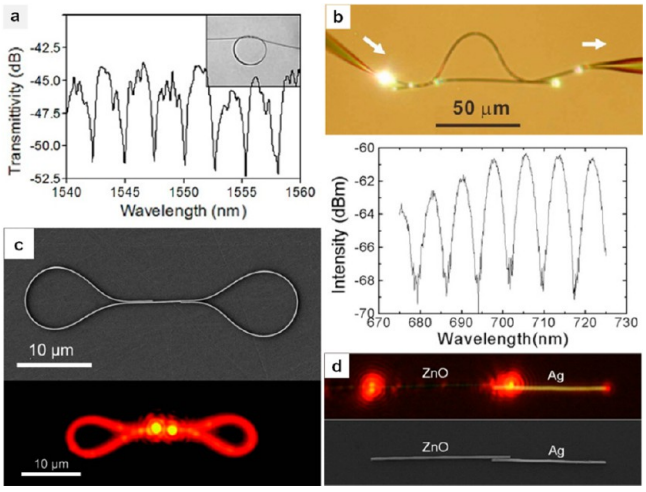

FIGURE 4. Functional nanowire assemblies. (a) Optical transmission spectrum and microscope image (inset) of a 150 μm diameter microring assembled with an 880 nm diameter silica nanowire. Adapted from ref 14 with permission. Copyright 2008 Elsevier. (b) Optical microscope image (top) and transmission spectrum (bottom) of a Mach–Zehnder structure assembled with two 480 nm diameter tellurite nanowires. Adapted from ref 37 with permission. Copyright 2008 Optical Society of America. (c) SEM (upper) and PL (bottom) images of a 200 nm diameter CdSe nanowire folded into microloops at both ends. Adapted from ref 25 with permission. Copyright 2011 American Chemical Society. (d) Optical microscope (top) and SEM (bottom) images of a hybrid photon–plasmon structure consisting of a 340 nm diameter ZnO nanowire and a 320 nm diameter Ag nanowire. Adapted from ref 38 with permission. Copyright 2009 American Chemical Society.

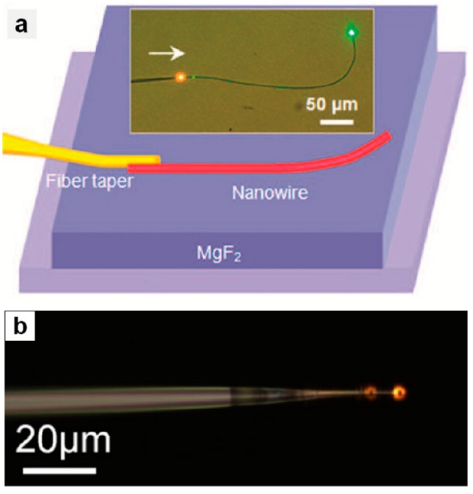

FIGURE 5. Optical launching of a single nanowire via a tapered fiber probe. (a) Schematic diagram and optical microscope image (inset) of launching a polymer nanowire supported on a MgF_2 substrate. Adapted from ref 17 with permission. Copyright 2008 American Chemical Society. (b) Optical microscope image of launching a 280 nm diameter Ag nanowire. Adapted from ref 40 with permission. Copyright 2013 Optical Society of America.

photon-to-plasmon coupling efficiency higher than 80% (Figure 5b).[38,40]

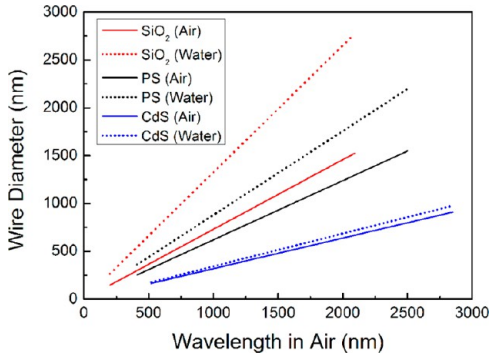

FIGURE 6. Single-mode cutoff diameters for typical nanowires in air (solid lines) and water (dotted lines). A nanowire with parameters beneath the corresponding line is single-mode.

4. Nanowire Optical Waveguides

Nanowire waveguiding at optical frequency can be categorized into two types: photonic waveguiding relying on electromagnetic response of bound electrons (e.g., in dielectrics) and plasmonic waveguiding relying on collective oscillation of quasi-free charges (e.g., in metals). For photonic applications, single-mode waveguiding is mostly preferred to avoid multimode interference. Single-mode condition for a free-standing photonic waveguiding nanowire is determined by

$$\pi\frac{D}{\lambda}(n_1{}^2 - n_2{}^2)^{1/2} < 2.405$$

where D is the nanowire diameter and n_1 and n_2 are refractive indices of the nanowire and the surrounding material, respectively.[5] As shown in Figure 6, to be a single-mode waveguide, the diameter of a typical nanowire should be close to or smaller than the wavelength of the light; while for a plasmonic waveguiding nanowire, there is no cutoff diameter for the TM modes, although coupling into the plasmon mode is very difficult when the nanowire is very thin.[41]

4.1. Evanescent Fields and Optical Confinement. By solving Maxwell's equations, one can obtain the field distribution of a waveguiding nanowire.[5] Figure 7 shows optical fields supported by typical photonic nanowires.[5,42] Compared with conventional optical waveguides that usually have a compromise between mode confinement and evanescent fields, a free-standing nanowire offers an opportunity to waveguide tightly confined optical fields with a high fraction of evanescent fields, which distinguishes the nanowire from many other waveguiding structures. For example, in Figure 7c, the 400 nm diameter nanowire guides a 633 nm wavelength light with about 30% power outside as evanescent waves, while it maintains an effective mode

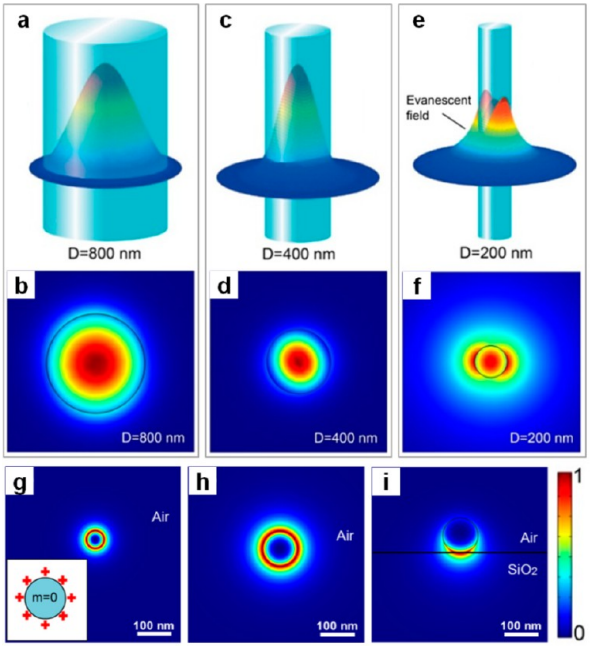

FIGURE 7. Spatial distributions of optical fields guided by nanowire waveguides. (a–f) Silica nanowire with diameter of (a, b) 800 nm, (c, d) 400 nm, and (e,f) 200 nm. Adapted from ref 5 with permission. Copyright 2004 Optical Society of America. (g–i) Au nanowire with diameters of (g) 50 nm and (h, i) 100 nm. The nanowire in panel I is supported on a silica substrate. Adapted from ref 42 with permission. Copyright 2012 Optical Society of America.

area of about 560 nm in diameter.[5] In Figure 7g, the 50 nm diameter Au nanowire confines 660 nm wavelength light into an effective mode area of about 0.0026 μm^2 ($\sim$0.006 λ^2), while leaving about 42% power outside as evanescent waves.[42]

4.2. Optical Loss. In a nonabsorptive nanowire, optical loss is usually contributed by radiation or scattering from the structural nonuniformities (e.g., surface roughness and defects), while in a metal nanowire, the absorption loss (Ohmic loss) is dominant. In Figure 8, we illustrate optical losses of typical photonic nanowires with corresponding effective mode areas. Owing to the ultralow surface roughness ($\sim$0.2 nm) and ultrahigh-purity preform (e.g., silica fiber), the taper-drawn silica nanowire can offer propagation loss as low as 0.001 dB/mm,[43] which is the lowest loss in subwavelength waveguides reported so far. Considering the intrinsic surface roughness of the capillary waves frozen during the drawing process, much lower optical loss of a glass nanowire is expected. Compared with the glass nanowire, a polymer nanowire usually has higher nonuniformities and consequently a higher optical loss. Crystalline semiconductor nanowires usually have similar surface roughness (down to atomic level) as the silica nanowires

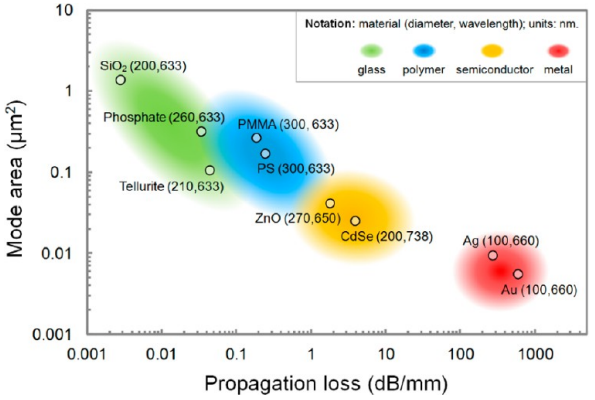

FIGURE 8. Optical losses of typical nanowires with corresponding effective mode areas.

but show much higher losses (>0.1 dB/mm). Several reasons are responsible: first, the higher index contrast (between the core material and the surrounding) of a semiconductor nanowire leading to a higher scattering loss;[44] second, the existence of band edge absorption; third, randomly distributed scattering centers (e.g., surface adsorption of debris) during the growth process. By improvement of the growth conditions or after treatments, much lower loss should be possible. As a subwavelength plasmonic waveguide, the Ag nanowire offers representatively low loss (e.g., 0.41 dB/μm at 633 nm wavelength),[33] although it is much higher than those of the dielectric nanowires. Coupling a metal nanowire with a dielectric substrate may enable hybrid plasmon modes with much lower losses, but the overall size of the waveguiding system is much larger than that of a free-standing nanowire. From the material aspect, searching better plasmonic materials may be a solution to free-standing low-loss plasmonic nanowires.[45]

4.3. Bandwidth and Diameter. The bandwidth for nanowire waveguiding depends on the material and waveguiding mechanisms. For dielectric and semiconductor nanowires, the short-wavelength edge is determined by the interband transition, while the long-wavelength edge is usually limited by either the optical confinement or the material absorption. Theoretically, no matter how thin a cylindrical waveguide is there is no cutoff of the fundamental mode.[46] However, in a real nanowire, when its diameter is far below the vacuum wavelength of the light, a slight disturbance to the geometric symmetry (e.g., intrinsic roughness or microbending) will lead to significant radiation loss, which sets an upper limit to the wavelength-to-diameter ratio (WDR) for a given nanowire. The maximum WDR for a free-standing silica nanowire is about 10,[47] which means that limited by the confinement, the longest allowed

wavelength is about 10 times the diameter. For a plasmonic nanowire with much tighter confinement, the maximum WDR could be larger. However, both the propagation and the coupling losses of the plasmonic nanowire increase with the increasing WDR,[42] which limits the available bandwidth.

5. Nanowire Optical Sensors

5.1. Motivation. The motivation of single-nanowire optical sensing comes from the increasing demand on miniaturized sensing platforms.[48] From the spatial aspect, the 1D nanowire not only provides tightly confined high-fractional evanescent fields for enhanced light–matter interaction, but also can offer the least path for routing light through the area to be measured, which enables sensing with small footprint, high spatial resolution, and low requirement for the sample volume. Meanwhile, an optical detection scheme exempts the parasitic response of electric circuits[10,11] and can be operated with fast response. Also, the low transverse dimension of the nanowire allows fast diffusion and evacuation of the specimen for fast and real-time detection. In addition, as the "beam size" (i.e., effective mode area) of a nanowire is very small (e.g., 500 nm), the driven power of a nanowire optical sensor can be extremely low, which is highly desired for safe detection of biochemical samples.

5.2. General Approaches. The mechanism of a typical nanowire sensor is schematically illustrated in Figure 9. Within the optical near field of a waveguiding nanowire, a slight fluctuation in dielectric constant may evidently modify the output of the nanowire by scattering, absorption, conversion, or re-emission of the guided light. By measurement of the intensity, phase, polarization, or spectrum of the output, the cause behind the fluctuation can be identified.

In most situations, the measurand is either spatially distributed or highly localized. For sensing spatially distributed samples, which are usually in forms of or dissolved in liquids or gases, the typical approach is measuring the refractive index or absorption, which directly reflect the change of measurands (e.g., concentration, temperature, or pressure). The high fractional evanescent fields that are directly exposed to the surrounding sample may greatly enhance the sensitivity of the nanowire sensor. For example, relying on phase-sensitive measurement of the index change, a nanowire Mach–Zehnder structure can offer a sensitivity 10 times higher than the conventional waveguide structures.[49] For absorptive samples, a direct intensity or spectral measurement can provide very high sensitivity and low detection limit. Recently, by embedding a 25 mm length silica nanowire in a microfluidic channel (Figure 10a–c) and measuring the spectral absorbance of the methylene blue (MB) around 630 nm wavelength, our group demonstrated a nanowire biochemical sensor with a detection limit of 50 pM and excellent reversibility (Figure 10d).[50] Using the same sensor for bovine serum albumin (BSA) measurement, we obtained a detection limit down to 20 fg/mL (Figure 10e). The sample required for the sensor is about 500 nL, and the probing light power is about 150 nW, suggesting a promising route to low-power high-sensitivity biochemical sensors.

For localized samples, for example, nanoparticles, the probing light guided by the nanowire can be confined to a "thin light beam" with size comparable to the particles, while maintaining strong evanescent fields for near-field interaction. In such a case, a particle with deep-subwavelength cross-section, which is imperceptible by ordinary light beams due to very low fractional scattering, can cause

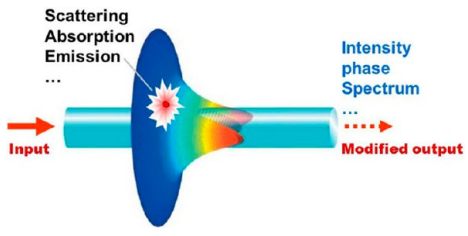

FIGURE 9. Schematic illustration of a waveguiding nanowire for optical sensing. The sample–light interaction (e.g., scattering, absorption, conversion, or re-emission) is reflected by the output (e.g., intensity, phase, or spectrum) of the nanowire.

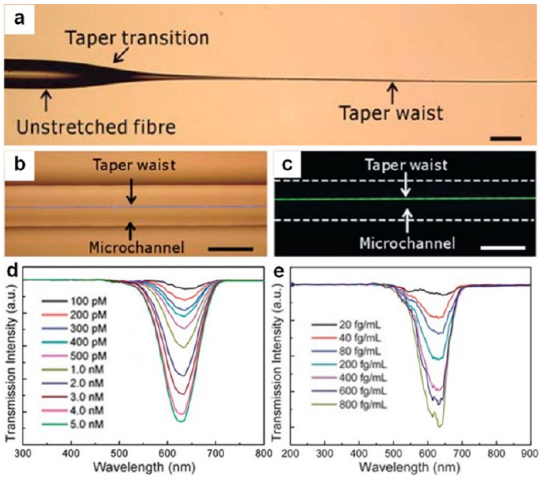

FIGURE 10. Integrated microfiber–microfluidic optical sensors. Optical microscope images of (a) a 900 nm diameter microfiber tapered down from a silica fiber, (b,c) an integrated microfiber–microfluidic structure before and after fluorescence excitation. All scale bars, 125 μm. (d,e) Transmission spectra of different (d) MB and (e) CB–BAS concentrations obtained using a 900 nm diameter microfiber. Adapted from ref 50 with permission. Copyright 2011 Royal Society of Chemistry.

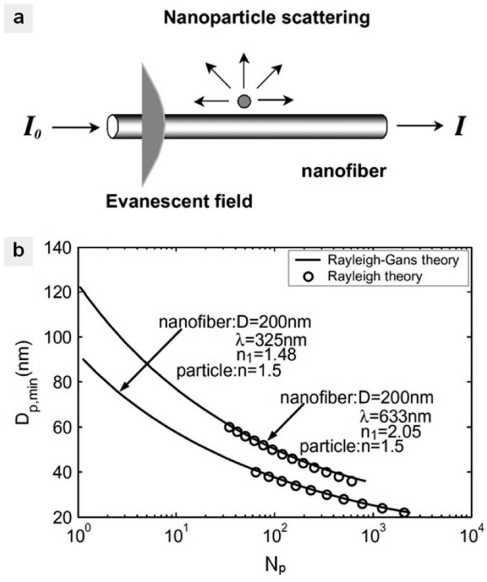

FIGURE 11. (a) Basic model of the light scattering of a nanoparticle in the vicinity of a nanowire. (b) The minimum required number (N_p) of particles for being detectable with respect to the particle diameter ($D_{p,min}$). The refractive index (n) of the particle and the diameter (D) of the fiber are assumed to be 1.5 and 200 nm, respectively. Adapted from ref 51 with permission. Copyright 2007 Elsevier.

detectable change to the transmission of a nanowire via evident scattering. For nonabsorptive particles, our calculation based on Rayleigh–Gans scattering theory showed that[51] with a 325 nm wavelength probing light guided in a 200 nm diameter silica nanowire, a single 90 nm diameter particle (index of 1.5) can be detected (Figure 11), indicating the possibility for single-molecule detection. Owing to the fast response of the optical detection, the surface adsorption of molecules have also been dynamically revealed.[52]

5.3. Material Functionalization. Activating a photonic nanowire by functional materials can offer great versatility for nanowire optical sensing. Here we use polymer nanowires as hosts due to their hospitability to a variety of dopants. Based on spectral response of an acidic-to-basic form change of bromothymol blue (BTB) doped in a 270 nm diameter poly(methyl methacrylate) (PMMA) nanowire, we demonstrated a nanowire NH_3 sensor with a detection limit of 3 ppm and a response time of about 1.8 s (Figure 12),[17] much faster than conventional ammonia sensors.[53] To activate the nanowire with high resistance to photobleaching, we doped CdSe/ZnS QDs into PS nanowires with QD concentration up to 10^4 μm^{-3},[34] and confirmed that the lifetime against the photobleaching of the QD-doped nanowire was 2 orders of magnitude longer than that of nanowires doped with dye molecules (Figure 13a). Based on

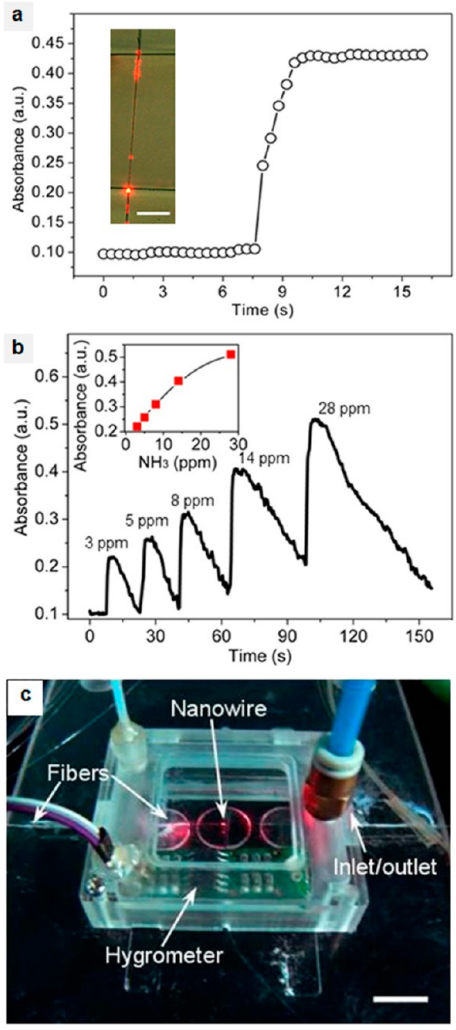

FIGURE 12. Chemical-indicator-doped nanowire optical sensor. (a) Optical response of a 270 nm diameter BTB-doped PMMA nanowire to 14 ppm NH_3 with a 660 nm wavelength light. Inset, optical micrograph of the sensing element. Scale bar, 50 μm. (b) Time-dependent absorbance of the nanowire to NH_3 gas cycled with concentrations from 3 to 28 ppm. Inset, dependence of the absorbance over the NH_3 concentration ranging from 3 to 28 ppm. (c) Prototype of the real single-nanowire optical sensor. Scale bar, 1 cm. Adapted from ref 17 with permission. Copyright 2008 American Chemical Society.

the surface passivation of QDs doped in a 480 nm diameter PS nanowire, a miniaturized optical humidity sensor (Figure 13b–d) was realized with a response time of 90 ms and a pumping power (532 nm CW light) down to 100 pW. More recently, by doping PAM nanowires with gold nanorods that were intrinsically stable against photobleaching, we observed a photon-to-plasmon-conversion efficiency as high as 70% for a single nanorod at 785 nm wavelength (Figure 14a–c),[35] and demonstrated a low-power fast-response optical humidity sensor that is intrinsically immune to photobleaching (Figure 14d–g).

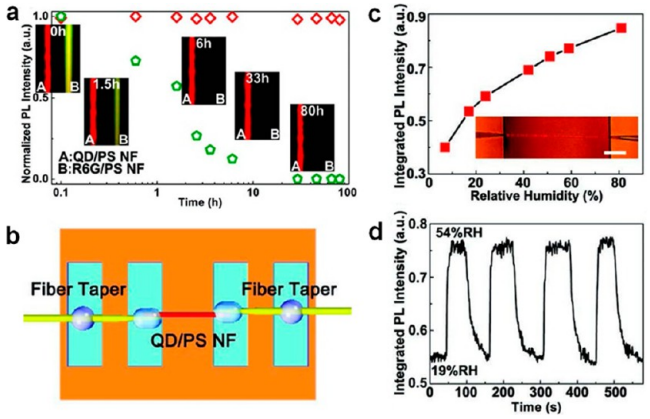

FIGURE 13. QD-doped nanowire optical sensor. (a) Time-dependent decay of the PL of a 580 nm diameter QD-doped PS nanowire (red diamond) and a 530 nm diameter R6G-doped PS nanowire (green pentagon). Insets: PL images of the two nanowires at different times. (b) Schematic illustration of a QD-doped PS nanowire optical sensor. (c) PL intensity of the nanowire exposed to ambient relative humidity (RH) ranging from 7% to 81%. Inset, optical microscopy image of the QD-doped nanowire sensing element. Scale bar: 50 μm. (d) Response of the nanowire sensor to alternately cycled 54% and 19% RH air. Adapted from ref 34 with permission. Copyright 2011 Wiley.

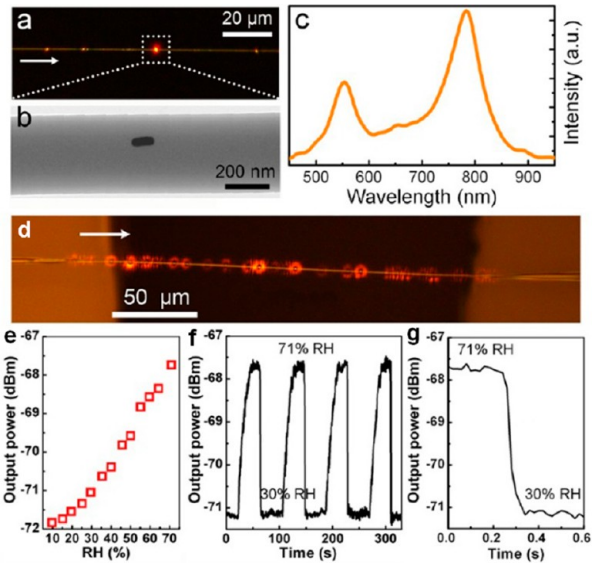

FIGURE 14. Au-nanoparticle-doped nanowire optical sensor. (a) Optical microscopy image of a 350 nm diameter single-Au-nanorod-doped PAM nanowire excited by a white light. (b) TEM image of the embedded nanorod. (c) Scattering spectrum of the waveguiding excited nanorod shown in panel a. (d) Optical microscopy image of a 540 nm diameter Au-nanorod-doped nanowire guiding a 785 nm wavelength light. (e) Output of the nanowire exposed to air of RH increasing from 9% to 71%. (f) Reversible response of the nanowire tested by cycling between 30% and 71% RH air. (g) A close-up view of the time-dependent response of the nanowire output. Adapted from ref 35 with permission. Copyright 2012 American Chemical Society.

5.4. Structural Functionalization. Structural functionalization is another promising approach to facilitating

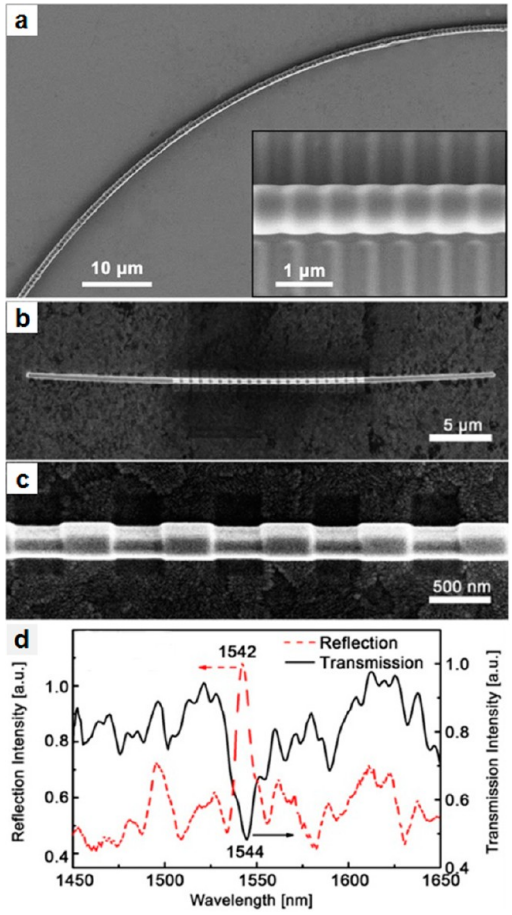

FIGURE 15. Micro- and nanowire optical gratings. (a) SEM image of a 900 nm diameter silica microfiber gratings. Inset, close-up view of the grating structures. Adapted from ref 55 with permission. Copyright 2011 Optical Society of America. (b,c) SEM images of gratings fabricated on a 290 nm diameter Au nanowire. (d) Normalized reflection and transmission spectra of the Au nanowire gratings. Adapted from ref 56 with permission. Copyright 2012 IOP Publishing.

nanowires for optical sensing. Similar to fiber grating technology, fabricating optical gratings on a single nanowire is also possible. Recently, high-sensitivity optical sensing using glass microfiber Bragg gratings has been demonstrated with fiber diameters down to 1 μm (Figure 15a),[54,55] which can be readily transplanted to nanowires of many other materials. For example, by focused-ion-beam milling of a 290 nm diameter Au nanowire, grating features with a transmission dip of ~3 dB are observed in merely 19 periods (totally 15.6 μm in length) (Figure 15b–d),[56] indicating an approach to ultracompact nanowire sensors based on plasmonic grating effects.

Besides, high-precision optical metrology can be adapted for nanowire sensing via functional assembly. For example, tying a nanowire into a ring to form a high-quality microcavity[13,14] or assembling two nanowires into a

Mach–Zehnder interferometer[37] may enable high-sensitivity measurement of optical phase or spectral shift on a miniaturized footprint. Incorporating these techniques into the nanowire sensor may greatly suppress the background fluctuation or noise (e.g., caused by drifting of surrounding temperature or pressure) and suggest a new approach to nanowire sensors with high accuracy and repeatability.

6. Future Outlook

So far, we have shown that nanowires are fascinating 1D structures for subwavelength waveguiding and optical sensing. Based on our initial attempts that addressed several critical issues such as efficient coupling of light into a nanowire and activating a nanowire by sensitive dopants, we have demonstrated single-nanowire optical sensors with high sensitivity, fast response, and low optical power, which may suggest a novel miniaturized sensing platform. However, a number of challenges remain, including (1) how to fabricate and functionalize nanowire structures with high repeatability, (2) how to protect the sensitive nanowire element from environmental contamination, (3) how to push the detection limit of a nanowire sensor to single-molecule level, and (4) more generally, for particular applications including optical sensing, how to balance or circumvent the interplay of loss, confinement, and bandwidth of a nanowire, which brings forth lasting challenges and opportunities for nanowire photonics, chemistry, and technology.

This work is supported by the National Basic Research Program of China (Grant No. 2013CB328703), the National Natural Science Foundation of China (Grant Nos. 61036012 and 61108048), the National Science and Technology Support Program (Grant No. 2012BAK08B05), and the Fundamental Research Funds for the Central Universities (Grant No. 2013QNA5005).

BIOGRAPHICAL INFORMATION

Xin Guo is a research associate professor in the Department of Optical Engineering at Zhejiang University. She received her Ph.D. from Zhejiang University (2010) with Dr. Limin Tong. Her current research interests include nanophotonics and plasmonics.

Yibin Ying is a professor in the College of Biosystems Engineering and Food Science at Zhejiang University. His research interests include chemical and biological nanosensors.

Limin Tong is a professor in the Department of Optical Engineering at Zhejiang University. He received his Ph.D. from Zhejiang University (1997). His group focuses on the area of nanophotonics and fiber optics. He is an Associate Editor of *Optics Express*.

FOOTNOTES

*Corresponding author. E-mail: phytong@zju.edu.cn.
The authors declare no competing financial interest.

REFERENCES

1 Yan, R. X.; Gargas, D.; Yang, P. D. Nanowire Photonics. *Nat. Photonics* **2009**, *3*, 569–576.
2 Tong, L. M.; Zi, F.; Guo, X.; Lou, J. Y. Optical Microfibers and Nanofibers: A Tutorial. *Opt. Commun.* **2012**, *285*, 4641–4647.
3 Lal, S.; Hafner, J. H.; Halas, N. J.; Link, S.; Nordlander, P. Noble Metal Nanowires: From Plasmon Waveguides to Passive and Active Devices. *Acc. Chem. Res.* **2012**, *45*, 1887–1895.
4 Cui, Q. H.; Zhao, Y. S.; Yao, J. N. Photonic Applications of One-Dimensional Organic Single-Crystalline Nanostructures: Optical Waveguides and Optically Pumped Lasers. *J. Mater. Chem.* **2012**, *22*, 4136–4140.
5 Tong, L. M.; Lou, J. Y.; Mazur, E. Single-Mode Guiding Properties of Subwavelength-Diameter Silica and Silicon Wire Waveguides. *Opt. Express* **2004**, *12*, 1025–1035.
6 She, W. L.; Yu, J. H.; Feng, R. H. Observation of a Push Force on the End Face of a Nanometer Silica Filament Exerted by Outgoing Light. *Phys. Rev. Lett.* **2008**, *101*, No. 243601.
7 Yu, J. H.; Feng, R. H.; She, W. L. Low-Power All-Optical Switch Based on the Bend Effect of a NM Fiber Taper Driven by Outgoing Light. *Opt. Express* **2009**, *17*, 4640–4645.
8 Xia, Y. N.; Yang, P. D.; Sun, Y. G.; Wu, Y. Y.; Mayers, B.; Gates, B.; Yin, Y. D.; Kim, F.; Yan, Y. Q. One-Dimensional Nanostructures: Synthesis, Characterization, and Applications. *Adv. Mater.* **2003**, *15*, 353–389.
9 Brambilla, G.; Payne, D. N. The Ultimate Strength of Glass Silica Nanowires. *Nano Lett.* **2009**, *9*, 831–835.
10 Cui, Y.; Wei, Q. Q.; Park, H. K.; Lieber, C. M. Nanowire Nanosensors for Highly Sensitive and Selective Detection of Biological and Chemical Species. *Science* **2001**, *293*, 1289–1292.
11 Huang, J. X.; Virji, S.; Weiller, B. H.; Kaner, R. B. Polyaniline Nanofibers: Facile Synthesis and Chemical Sensors. *J. Am. Chem. Soc.* **2003**, *125*, 314–315.
12 Lee, B. Review of the Present Status of Optical Fiber Sensors. *Opt. Fiber Technol.* **2003**, *9*, 57–79.
13 Tong, L. M.; Gattass, R. R.; Ashcom, J. B.; He, S. L.; Lou, J. Y.; Shen, M. Y.; Maxwell, I.; Mazur, E. Subwavelength-Diameter Silica Wires for Low-loss Optical Wave Guiding. *Nature* **2003**, *426*, 816–819.
14 Tong, L. M.; Mazur, E. Glass Nanofibers for Micro- and Nano-Scale Photonic Devices. *J. Non-Cryst. Solids* **2008**, *354*, 1240–1244.
15 Tong, L. M.; Hu, L. L.; Zhang, J. J.; Qiu, J. R.; Yang, Q.; Lou, J. Y.; Shen, Y. H.; He, J. L.; Ye, Z. Z. Photonic Nanowires Directly Drawn from Bulk Glasses. *Opt. Express* **2006**, *14*, 82–87.
16 Harfenist, S. A.; Cambron, S. D.; Nelson, E. W.; Berry, S. M.; Isham, A. W.; Crain, M. M.; Walsh, K. M.; Keynton, R. S.; Cohn, R. W. Direct Drawing of Suspended Filamentary Micro- and Nanostructures from Liquid Polymers. *Nano Lett.* **2004**, *4*, 1931–1937.
17 Gu, F. X.; Zhang, L.; Yin, X. F.; Tong, L. M. Polymer Single-Nanowire Optical Sensors. *Nano Lett.* **2008**, *8*, 2757–2761.
18 Gu, F. X.; Yu, H. K.; Wang, P.; Yang, Z. Y.; Tong, L. M. Light-Emitting Polymer Single Nanofibers via Waveguiding Excitation. *ACS Nano* **2010**, *4*, 5332–5338.
19 Xing, X. B.; Zhu, H.; Wang, Y. Q.; Li, B. J. Ultracompact Photonic Coupling Splitters Twisted by PTT Nanowires. *Nano Lett.* **2008**, *8*, 2839–2843.
20 Pan, Z. W.; Dai, Z. R.; Ma, C.; Wang, Z. L. Molten Gallium as a Catalyst for the Large-Scale Growth of Highly Aligned Silica Nanowires. *J. Am. Chem. Soc.* **2002**, *124*, 1817–1822.
21 Hu, J. Q.; Meng, X. M.; Jiang, Y.; Lee, C. S.; Lee, S. T. Fabrication of Germanium-Filled Silica Nanotubes and Aligned Silica Nanofibers. *Adv. Mater.* **2003**, *15*, 70–73.
22 Li, D.; Xia, Y. N. Fabrication of Titania Nanofibers by Electrospinning. *Nano Lett.* **2003**, *3*, 555–560.
23 Lu, X. F.; Wang, C.; Wei, Y. One-Dimensional Composite Nanomaterials: Synthesis by Electrospinning and Their Applications. *Small* **2009**, *5*, 2349–2370.
24 Morales, A. M.; Lieber, C. M. A Laser Ablation Method for the Synthesis of Crystalline Semiconductor Nanowires. *Science* **1998**, *279*, 208–211.
25 Xiao, Y.; Meng, C.; Wang, P.; Ye, Y.; Yu, H. K.; Wang, S. S.; Gu, F. X.; Dai, L.; Tong, L. M. Single-Nanowire Single-Mode Laser. *Nano Lett.* **2011**, *11*, 1122–1126.
26 Gudiksen, M. S.; Lauhon, L. J.; Wang, J.; Smith, D. C.; Lieber, C. M. Growth of Nanowire Superlattice Structures for Nanoscale Photonics and Electronics. *Nature* **2002**, *415*, 617–620.
27 Gu, F. X.; Yang, Z. Y.; Yu, H. K.; Xu, J. Y.; Wang, P.; Tong, L. M.; Pan, A. L. Spatial Bandgap Engineering along Single Alloy Nanowires. *J. Am. Chem. Soc.* **2011**, *133*, 2037–2039.
28 Dick, K. A.; Deppert, K.; Larsson, M. W.; Martensson, T.; Seifert, W.; Wallenberg, L. R.; Samuelson, L. Synthesis of Branched `Nanotrees' by Controlled Seeding of Multiple Branching Events. *Nat. Mater.* **2004**, *3*, 380–384.

29 Yan, H. Q.; He, R. R.; Johnson, J.; Law, M.; Saykally, R. J.; Yang, P. D. Dendritic Nanowire Ultraviolet Laser Array. *J. Am. Chem. Soc.* **2003**, *125*, 4728–4729.

30 Zhao, X. Y.; Wei, C. M.; Yang, L.; Chou, M. Y. Quantum Confinement and Electronic Properties of Silicon Nanowires. *Phys. Rev. Lett.* **2004**, *92*, No. 236805.

31 Ditlbacher, H.; Hohenau, A.; Wagner, D.; Kreibig, U.; Rogers, M.; Hofer, F.; Aussenegg, F. R.; Krenn, J. R. Silver Nanowires as Surface Plasmon Resonators. *Phys. Rev. Lett.* **2005**, *95*, No. 257403.

32 Sun, Y. G.; Xia, Y. N. Large-Scale Synthesis of Uniform Silver Nanowires through a Soft, Self-Seeding, Polyol Process. *Adv. Mater.* **2002**, *14*, 833–837.

33 Ma, Y. G.; Li, X. Y.; Yu, H. K.; Tong, L. M.; Gu, Y.; Gong, Q. H. Direct Measurement of Propagation Losses in Silver Nanowires. *Opt. Lett.* **2010**, *35*, 1160–1162.

34 Meng, C.; Xiao, Y.; Wang, P.; Zhang, L.; Liu, Y. X.; Tong, L. M. Quantum-Dot-Doped Polymer Nanofibers for Optical Sensing. *Adv. Mater.* **2011**, *23*, 3770–3774.

35 Wang, P.; Zhang, L.; Xia, Y. N.; Tong, L. M.; Xu, X.; Ying, Y. B. Polymer Nanofibers Embedded with Aligned Gold Nanorods: A New Platform for Plasmonic Studies and Optical Sensing. *Nano Lett.* **2012**, *12*, 3145–3150.

36 Yalla, R.; Kien, F. L.; Morinaga, M.; Hakuta, K. Efficient Channeling of Fluorescence Photons from Single Quantum Dots into Guided Modes of Optical Nanofiber. *Phys. Rev. Lett.* **2012**, *109*, No. 063602.

37 Li, Y. H.; Tong, L. M. Mach–Zehnder Interferometers Assembled with Optical Microfibers or Nanofibers. *Opt. Lett.* **2008**, *33*, 303–305.

38 Guo, X.; Qiu, M.; Bao, J. M.; Wiley, B. J.; Yang, Q.; Zhang, X. N.; Ma, Y. G.; Yu, H. K.; Tong, L. M. Direct Coupling of Plasmonic and Photonic Nanowires for Hybrid Nanophotonic Components and Circuits. *Nano Lett.* **2009**, *9*, 4515–4519.

39 Huang, K. J.; Yang, S. Y.; Tong, L. M. Modeling of Evanescent Coupling between Two Parallel Optical Nanowires. *Appl. Opt.* **2007**, *46*, 1429–1434.

40 Li, X. Y.; Li, W.; Guo, X.; Lou, J. Y.; Tong, L. M. All-Fiber Hybrid Photon-Plasmon Circuits: Integrating Nanowire Plasmonics with Fiber Optics. *Opt. Express* **2013**, *21*, 15698–15705.

41 Chang, D. E.; Sørensen, A. S.; Hemmer, P. R.; Lukin, M. D. Strong Coupling of Single Emitters to Surface Plasmons. *Phys. Rev. B* **2007**, *76*, No. 035420.

42 Wang, Y. P.; Ma, Y. G.; Guo, X.; Tong, L. M. Single-Mode Plasmonic Waveguiding Properties of Metal Nanowires with Dielectric Substrates. *Opt. Express* **2012**, *20*, 19006–19015.

43 Brambilla, G.; Finazzi, V.; Richardson, D. J. Ultra-Low-Loss Optical Fiber Nanotapers. *Opt. Express* **2004**, *12*, 2258–2263.

44 Poulton, C. G.; Koos, C.; Fujii, M.; Pfrang, A.; Schimme, T.; Leuthold, J.; Freude, W. Radiation Modes and Roughness Loss in High Index-Contrast Waveguides. *IEEE J. Quantum Electron.* **2006**, *12*, 1306–1321.

45 West, P. R.; Ishii, S.; Naik, G. V.; Emani, N. K.; Shalaev, V. M.; Boltasseva, A. Searching for Better Plasmonic Materials. *Laser Photon. Rev.* **2010**, *4*, 795–808.

46 Snyder, A. W.; Love, J. D. *Optical Waveguide Theory*; Chapman and Hall: New York, NY, 1983.

47 Sumetsky, M. How Thin Can a Microfiber Be and Still Guide Light? *Opt. Lett.* **2006**, *31*, 870–872.

48 Sirbuly, D. J.; Tao, A.; Law, M.; Fan, R.; Yang, P. D. Multifunctional Nanowire Evanescent Wave Optical Sensors. *Adv. Mater.* **2007**, *19*, 61–66.

49 Lou, J. Y.; Tong, L. M.; Ye, Z. Z. Modeling of Silica Nanowires for Optical Sensing. *Opt. Express* **2005**, *13*, 2135–2140.

50 Zhang, L.; Wang, P.; Xiao, Y.; Yu, H. K.; Tong, L. M. Ultra-Sensitive Microfibre Absorption Detection in a Microfluidic Chip. *Lab Chip* **2011**, *11*, 3720–3724.

51 Wang, S. S.; Pan, X. Y.; Tong, L. M. Modeling of Nanoparticle-Induced Rayleigh-Gans Scattering for Nanofiber Optical Sensing. *Opt. Commun.* **2007**, *276*, 293–297.

52 Warken, F.; Vetsch, E.; Meschede, D.; Sokolowski, M.; Rauschenbeutel, A. Ultra-Sensitive Surface Absorption Spectroscopy Using Sub-Wavelength Diameter Optical Fibers. *Opt. Express* **2007**, *15*, 11952–11958.

53 Cao, W. Q.; Duan, Y. X. Optical Fiber-Based Evanescent Ammonia Sensor. *Sens. Actuators, B* **2005**, *11*, 252–259.

54 Fang, X.; Liao, C. R.; Wang, D. N. Femtosecond Laser Fabricated Fiber Bragg Grating in Microfiber for Refractive Index Sensing. *Opt. Lett.* **2010**, *35*, 1007–1009.

55 Liu, Y. X.; Meng, C.; Zhang, A. P.; Xiao, Y.; Yu, H. K.; Tong, L. M. Compact Microfiber Bragg Gratings with High-Index Contrast. *Opt. Lett.* **2011**, *36*, 3115–3117.

56 Zhang, X. N.; Ma, Z.; Luo, R.; Gu, Y.; Meng, C.; Wu, X. Q.; Gong, Q. H.; Tong, L. M. Single-Nanowire Surface Plasmon Gratings. *Nanotechnology* **2012**, *23*, No. 225202.